12th International Conference on Hydroinformatics, HIC 2016

Determination of Wave Reflection Formulae for Vertical and Sloped Seawalls Via Experimental Modelling

Abdelazim Negm[a,*] , Karim Nassar[b]

[b]*Head of Natural Resources Lab., Environmental Engineering Department, Egypt-Japan University of Science and Technology, E-JUST, Alexandria, Egypt (Seconded from Faculty of Engineering, Zagazig University, Zagazig, Egypt)*

[a] *PhD student in Environmental Engineering Department, School of Energy and Environmental Engineering, Egypt-Japan University of Science and Technology, E-JUST, P.O.Box 179, New Borg Al-Arab City, Postal Code 21934, Alexandria, Egypt.*

Abstract

This paper presents and discusses the results of experimental investigations using both vertical and sloping seawalls configurations to determine the optimal wave reflection characteristics of seawalls for protecting beaches against erosion under a variety of hydrodynamic conditions. The different experiments include both of rectangular or triangular serrated blocks and slotted seawalls with or without triangular serrations as energy dissipaters. The linear wave theory is utilized. Moreover, the Dalrymple method is considered to predict the ordinates of the resultant standing wave due to the partial wave reflection. Using the dimensional analysis, lab measurements, and SPSS, predictive formulae are proposed to predict the reflection coefficient for the five tested models by using SPSS software. The findings of the present investigation could be applied to optimize the design criteria of shore protection structures.

Keywords: Wave Reflection; Dalrymple method; Wave breaking; Seawalls; Iribarin number; SPSS.

1. Introduction

Seawalls are constructed parallel to the coastline to provide a great defense against flooding of coastal low-land areas and to protect the shore from excessive erosion while also immobilizing the sand of the adjacent beach.

———————

* Corresponding author.
E-mail address: negm@ejust.edu.eg

* First author. Tel.:+2-010-9811-8002, +2-0100-573-5345 fax +203-459-9520
E-mail address: karim.nassar@ejust.edu.eg, negm@ejust.edu.eg

To properly design seawalls detailed information is required on various wave hydrodynamics, configuration of the area to be protected and degree of severity. Some theoretical and experimental investigations on different hydrodynamic aspects on vertical as well as sloped seawalls were reported in the literature.

[1] Presented numerical solutions for the wave reflection from submerged porous structures in front of the impermeable vertical seawall. [2] Studied the solitary wave interaction with fully emerged rectangular porous seawalls by using a two-dimensional numerical model. [3] Developed a new formula using a large experimental data of the reflection coefficients for permeable and impermeable seawalls. [4] Investigated experimentally a new type of wave absorbing quay-wall with a partial wave chamber containing a rock-armored slope. The wave reflection characteristics of a porous seawall that might be used in protecting coasts from probable sea level rising were experimentally studied using physical models by [5]. The hydrodynamic performance of both vertical and sloped seawalls was investigated experimentally by [6] using physical model studies under regular waves of a wide range of heights, and periods. A critical review of the existing literature reveals that the vertical seawalls have the disadvantage of increasing the water particle kinematics in front of the structure due to significant wave reflection, which results in increased wave loads on the seawall and increased toe scour. To overcome this difficulty, sloped seawalls had been introduced. Sloped seawalls are good energy dissipaters when compared to vertical seawalls, especially when the slope of the seawall becomes milder. Sloped seawalls cause a phase lag of reflected waves and induce waves to break on the slope by spilling and hence dissipate a part of the incident wave energy [6]. However, milder the slope of the seawall, the more expensive is. Therefore, sloped seawalls of different angles with the seabed with energy dissipaters in the form of rectangular or triangular serrated blocks, and horizontally slotted with triangular serrations or without any serrations are examined experimentally in this study.

Nomenclature	
a, and b	Constants used in formulae for determination of wave reflection coefficient
d	Still water depth
G	Slots ratio per $1.0\ m^2$
H_i	Incident wave height
H_o	Deep zone wave height
H_r	Reflected wave height
K_r	Reflection coefficient
L_i	Incident wave length
L_o	Deep zone wave length
P_1, P_2, P_3	Wave recorders
s	Net spacing between dissipater blocks
T	Wave period
w	Width of dissipater blocks in the direction of wall slope
θ	Slope angle between seawall and seabed
α	Sea bed angle
$\eta(x)$	Water elevation above still water level at location (x) from wall toe
η_{max}	Maximum water elevation above still water level
η_{min}	Minimum water elevation above still water level
β	Angle of wave attack
ξ	Surf similarity parameter (Iribarren number)
SPSS	Statistical Package for Social Science
SWL	Still Water Level

2. Experimental Setup

Several experiments are carried out in a wave flume 15.1m long, 1.0m wide and 1.0m depth. A flap type wave

generator is used to displace the water in the flume to get the desired wave characteristics. This wave generator is installed at one end of the flume. Two wave absorbers are used to prevent the reflection of waves at the other end of the flume in order to increase the efficiency of experiments and to reduce the time required between runs while the water is calming down. The first absorber is placed in the front of the wave generator, while the other absorber is installed at the end of the flume with a slope of 1:7 as recommended by [7]. The experiments are carried out with a constant water depth, d, of 0.4 m. The flap is controlled by an induction motor of 11 kW. This motor is regulated by an inventor drive (0-50Hz) rotating in a speed range of 0-155 rpm. Regular waves of heights, H_i, (6.495 to11.1cm) of periods, T, (0.669 to 1.308s) have been generated with this facility.

2.1 Model Details

Five different types of the seawalls are examined covering different structural and wave conditions (i.e. plane seawall, plane wall with rectangular serrations, plane wall with triangular serrations, slotted seawall, and slotted seawall with triangular serrations) as shown in Fig. 1a.
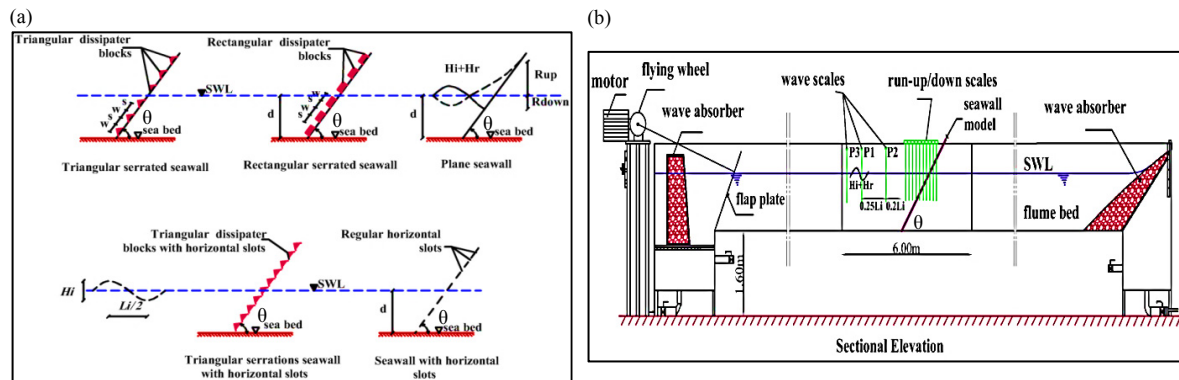

Fig. 1. (a) Definition sketches of seawall physical models; (b) Sectional elevation for the used wave flume..

The tested models are placed at the middle of the wave flume. The models are fixed inside the wave flume rigidly for the required angle of inclination (i.e. θ = 45, 60, 75 and 90⁰) by using supports and wedges driven between the model and flume wall. The models consist of a plane plate, rectangular, and triangular dissipater blocks. Plate made of hardwood of thick 3mm coated with water insulation material. Blocks are made of wood of sizes 99cm length, 5 cm width (parallel to wall slope), 4cm height (perpendicular on wall slope). They are fixed in a regular manner. The leakage of water between the model and the flume wall has been sealed by wooden planks.

Table 1. Range of governing variables.

Variable	Symbol	Unit	Range
Water depth	d	cm	40.0
Inventor frequency	-	Hz	From 2.5 to 4.9
Wave periods	T	sec	From 0.669 to1.308
Wave heights	H_i	cm	From 6.495 to 11.1
deep zone wave height	H_o	cm	From 5.93 to 11.093
Incident wave length	L_i	cm	From 69.69 to 218.4
Deep zone wave length	L_o	cm	From 69.82 to 266.89
Angle of wave attack	β	-	90º
Seabed angle	α	-	0º
Dissipater blocks spacing	s	cm	5.0, 10, and 15
Dissipater block width in the direction of seawall slope	w	Cm	5.0
Slots ratio	G	-	0.13, 0.23, and 0.33 per 1 m²
Seawall slopes	θ	-	45, 60, 75, and 90º

2.2. Parameters identification

A dimensional analysis using Buckingham Pi theorem is performed in order to develop relationships of K_r in terms of hydraulic and geometrical characteristics of the suggested models. The analysis presents the hydrodynamic performance in front of the seawall in terms of relationships between reflection coefficient, *Kr*, and the dimensionless parameters that represent the wave and structure characteristics as in the following equation:

$$K_r = f\left(\frac{H_i}{L_i}, \xi, \frac{d}{L_i}, \frac{s}{w}, G, \cot\theta\right) \tag{1}$$

The governing variables and their possible range of application are illustrated in Table 1, while the hydrodynamic performance of the tested seawalls have been checked in response to non-dimensional seawall and wave characteristic parameters as presented in Equation 1 and are listed in Table 2.

Table 2. Range of non-dimensional seawall and wave characteristics:

Parameter	Range
Relative wave depth (d/L_i)	From 0.183 to 0.574
Wave steepness (H_i/L_i)	From 0.0297 to 0.1593
Surf similarity parameter (ξ)	From 2.426 to 2.932 (plunging wave)
	From 3.394 to 23.924 (surging wave)
Relative dissipater blocks spacing (s/w)	1.0, 2.0, and 3.0
Slots ratio for 1.0 m^2(G)	0.13, 0.23, and 0.33
Cot θ	0, 0.267, 0.577, and 1.0

2.3 Instrumentation

2.3.1. Wave scales

Vertical scales fixed with the Perspex part are used to measure the wave characteristics (i.e. P1, P2, and P3), see Fig. 1b. The accuracy of these scales is 1.0 mm. The vertical scale is selected to be in front of the seawall model (seaward side) to measure the hydrodynamic parameter of waves (i.e. incident wave height, and wave reflected height).

2.3.2. Data acquisition

A digital camera (e.g. auto focus 21 mega pixel, and optical zoom 5 x) is used for recording the wave characteristics. It is connected to a personal computer, in order to analyze the wave data. The camera is exactly adjusted perpendicular to the required vertical scale then fixed on a vertical stand on horizontal table to avoid vibrations during shots. The water level variation which resulted from the wave action is recorded by a camera for various frequencies, ranging from 2.5Hz to 4.9Hz, at the selected measuring points. These data are converted to the wave elevations by simple computer program, and then the variation of water surface with time is plotted.

2.3.3. Incident, and reflected wave heights

The incident wave heights (Hi) are measured by using the wave probe P3. The values of the incident wave heights which calculated according to the method of [8], are compared to those measured using wave probe P3. These values agreed quite closely (i.e. R-squared value equal to 0.977).

To separate the incident (Hi) and reflected (Hr) wave heights, two probes P2 and P1 (max. at location P1, the quasi-antinodes, and min. at location P2, the quasi-nodes) are set in front of the model at distances 0.2 L_i and 0.45 L_i respectively (L_i is the local incident wave length) measured from seawall toe according to [8]. The incident wavelength L_i is variable according to the wave period T, where it calculated by using the dispersion relationship according to the linear wave theory.

The water elevation η(x) for any location x, can be estimated by [8] as follows:

$$\eta(x) = \pm\sqrt{(H_i/2)^2 + (H_r/2)^2 + (H_i H_r/2)\cos(2kx + \varepsilon)} \tag{2}$$

In which, (k) is the wave number ($k=2\pi/L_i$) and (ε) is the phase lag induced by the reflection process. The η(x) obviously varies periodically with (x) and it becomes a maximum of the envelope at the phase positions,

$(2kx_1+\varepsilon) = 2n\pi,\ n=0, 1, 2, \ldots$ (3)

$\eta(x)_{max.} = (H_i+H_r)/2$ (the quasi-antinodes) (4)

Whereas at the phase positions,

$(2kx_2+\varepsilon) = (2n+1)\pi,\ n= 0, 1, 2,\ \ldots$ (5)

It becomes a minimum of the envelope:

$\eta(x)_{min.} = (H_i - H_r) / 2$ (the quasi-nodes) (6)

It is easy to obtain the actual distance between vertical scales P_1 and P_2 by subtracting Equation 5 from Equation 3, so it will be equal to $L_i/4$.
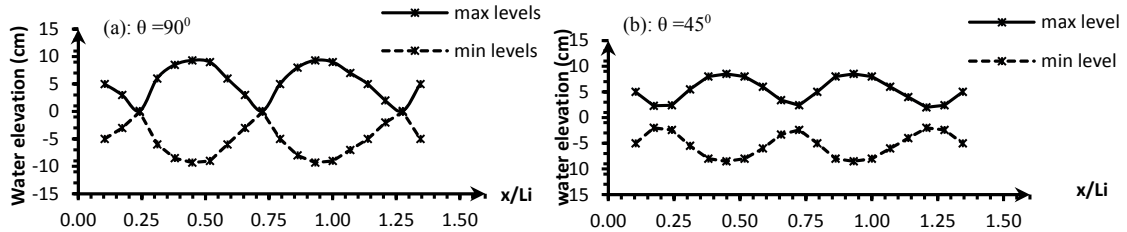

Fig. 2. Partial standing wave envelope for the case of plane seawall at (H_i=9.4 cm, L_i=144.7cm , and T=0.994 sec).
(a) θ=90^0; (b) θ=45^0.

To verify this, a typical envelope of the partial standing wave induced by a plane wall (for slope angles (θ) = 90^0, and 45^0, L_i=144.7cm , H_i=9.4cm, T= 0.994 sec) are measured and plotted in Figures 2a, and 2b. In this figure, maximum and minimum wave elevations measured at different spatial positions along the wave flume at 0.1m intervals from x=0.15 to1.95m are given. In a partial standing wave field, nodes and antinodes alternate spatially at x-locations at increments of $L_i/4$.

The calculated incident (H_i) and reflected (H_r) wave heights estimated from Equations (4) and (6) as:

$$H_i = \eta_{max} + \eta_{min} = \frac{H_{max} + H_{min}}{2}$$
(7)

$$H_r = \eta_{max} - \eta_{min} = \frac{H_{max} - H_{min}}{2}$$
(8)

Where:

H_{max} = max wave height (at antinodes) = max crest level - min through level; and

H_{min} = min wave height (at nodes) = min crest level-max through level.

The reflection coefficient, K_r, is the ratio between reflected and incident wave heights, therefore:

$$K_r = \frac{H_r}{H_i}$$
(9)

$$K_r = \frac{H_{max} - H_{min}}{H_{max} + H_{min}}$$
(10)

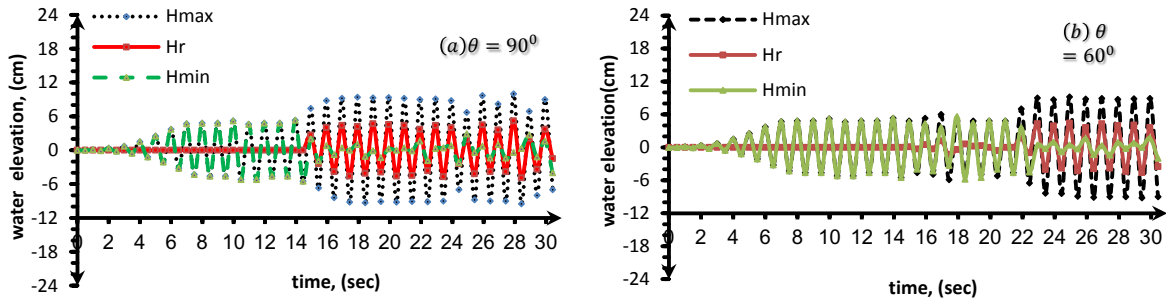Fig. 3.Typical time series of the variation of water levels for the standing wave obtained from plane wall (H$_i$=9.4 cm, L$_i$=144.7cm , and T=0.994s) (a) θ=90^0; (b) θ=60^0.

A typical time series for the variation of water levels for the standing wave obtained from plane wall at different wall slopes (H$_i$=9.4 cm, L$_i$=144.7cm , and T=0.994 sec) is presented in Fig. 3. As shown from Fig. 3a, the standing wave begins to start after 16 seconds in the case of slope angle 90^0, while it begins to start after 23 sec for slope angle 60^0 as presented in fig. 3b. It is noticed that whenever the slope become milder, the occurrence of the standing waves become more late. This lag of time occurs due to the excessive dissipation of energy for the waves on the seawalls slopes due to wave breaking.

3. Predictive Equations

Based on the above dimensionless parameters in Equation 1, a non-linear regression analysis is carried out on about 70% of the observed data using SPSS [9] to obtain predictive equations for estimating the values of K$_r$ as follow:

$$K_r = a_1 \left(\frac{d}{L_i} \right)^{b_1} \left(\frac{H_i}{L_i} \right)^{c_1} \left(\xi \right)^{d_1} \left(\cot \theta \right)^{e_1} \left(\frac{s}{w} \right)^{f_1} \left(G \right)^{g_1} \tag{11}$$

The values of the parameters, a$_1$, b$_1$, c$_1$, d$_1$, e$_1$, f$_1$, and g$_1$ for plane, rectangular serrated, triangular serrated seawall, slotted seawall, and slotted seawall with triangular serrations in case of vertical and sloped wall faces are listed in Table 3.

Table 3. Estimated parameters of equation 11 for predicting wave reflection for different seawall types.

Vertical seawall (cot θ = 0.0)							
Wall type	a$_1$	b$_1$	c$_1$	d$_1$	e$_1$	f$_1$	g$_1$
1-Plane, R^2= 0.91	0.92	0.05	-0.04	0.0	0.0	0.0	0.0
2-Rectangular Serrated, R^2= 0.55	0.4	0.33	-.039	0.0	0.0	-0.03	0.0
3-Triangular serrated, R^2= 0.5	0.48	0.17	-0.25	0.0	0.0	0.03	0.0
4-Slotted, R^2=0.99	0.4	0.02	-0.02	0.0	0.0	0.0	-0.3
5-Slotted + triangular serrations, R^2=0.99	0.4	-0.05	0.01	0.0	0.0	0.0	-0.3
Sloped seawall (cot θ from 0.267 to 1.0)							
Wall type	a$_1$	b$_1$	c$_1$	d$_1$	e$_1$	f$_1$	g$_1$
1-Plane, R^2= 0.82	0.51	-0.1	-0.48	-0.76	-1.0	0.0	0.0
2-Rectangular Serrated, R^2= 0.78	0.25	0.06	-0.82	-1.0	-1.3	-0.06	0.0
3-Triangular serrated, R^2= 0.74	0.31	-0.07	-0.61	-0.8	-1.1	0.04	0.0
4-Slotted, R^2=0.9	0.29	-0.34	0.9	1.4	1.2	0.0	-0.4
5-Slotted + triangular serrations, R^2=0.9	0.25	-0.34	0.94	1.48	1.3	0.0	-0.4

3.1. Data verification

The remaining 30% of the observed data are used to verify the predicted values of K$_r$ which obtained from Equation 11.
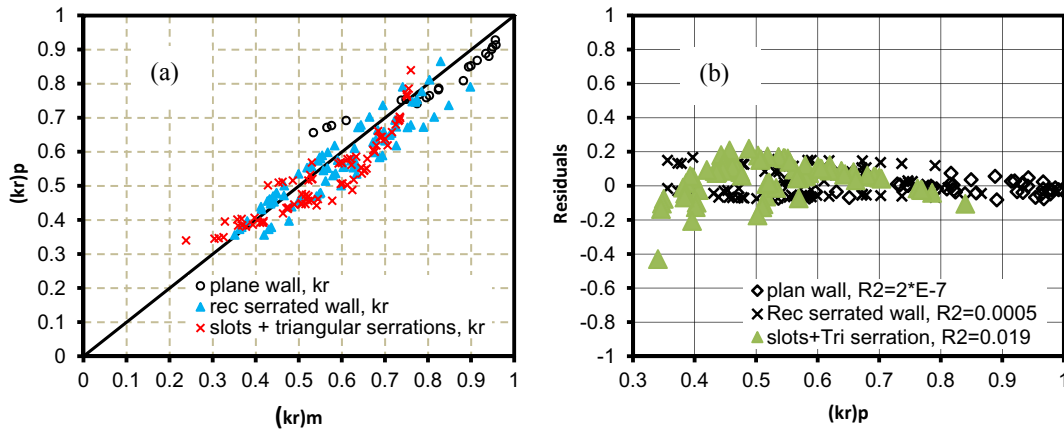
Fig. (4). Residuals and comparison between the measured and predicted wave reflection coefficient for the sloped plane, rectangular serrated, and slotted with triangular serrations walls by using nonlinear regression. (a): wave reflection coefficient, (b): residuals of wave reflection coefficient.

The data points are reasonably distributed on either side of a 45° line which is used for observing the correlation between the predicted and observed K_r. Fig. 4a is plotted to depict the correlation between the measured and predicted values of K_r for the plane wall, rectangular serrated wall, and slotted wall with triangular serration for the sloped case. As well fig. 4b demonstrates the residuals and the corresponding mean square errors for the predicted values of K_r based on Equation 11.

As depicted through fig.4, the values of correlation factor for K_r are 2×10^{-7}, 0.0005, 0.019 for plane, rectangular serrated, and slotted with triangular serrations respectively. It is noticed that the agreement between observed and predicted values is slightly converged. Also, the values of residuals are found rather small with negligible correlation coefficient and symmetrically distributed around the line of zero error.

3.2. Data validation

The empirical equations are validated by comparison with previous predictions and experiments for the limiting cases of the seawall. Fig. 5 describes a comparison between the results of present work (i.e. vertical plane impermeable seawall, vertical rectangular serrated seawall, s/w=2.0, and vertical triangular serrated seawall, s/w=2.0) and the results of other authors and formulae for predicting the wave reflection coefficient for vertical impermeable seawalls. The different formulae which used for predicting the values of K_r at wave periods (i.e. $d/L_i = 0.183$ to 0.574), wave steepness (i.e. $H_i/L_i = 0.0297$ to 0.1593) are described as follow:

Vertical plane seawall (present study):

$$kr = 0.919 \left(\frac{d}{L_i} \right)^{0.054} \left(\frac{H_i}{L_i} \right)^{-0.049} \tag{12}$$

Vertical rectangular serrated seawall (present study):

$$kr = 0.401 \left(\frac{d}{L_i} \right)^{0.334} \left(\frac{H_i}{L_i} \right)^{-0.389} \left(\frac{s}{w} \right)^{-0.027} \tag{13}$$

Vertical triangular serrated seawall (present study):

$$kr = 0.485 \left(\frac{d}{L_i} \right)^{0.172} \left(\frac{H_i}{L_i} \right)^{-0.249} \left(\frac{s}{w} \right)^{0.032} \tag{14}$$

After [5]: $kr = 0.83 \left(\frac{d}{L_i} \right)^{0.16} \left(\frac{H_i}{L_i} \right)^{-0.12}$ $\tag{15}$

After [10]: $kr = 0.66 + \left[\dfrac{0.22}{d/L_i}\right]$ (for serrated wall)   (16)

and, $kr = \dfrac{d}{L_i}\left[1.5\left(\dfrac{d}{L_i}\right) - 0.03\right]$ (for dentated wall)   (17)

The figure shows that for vertical smooth impermeable seawalls obtained by present study, [5], and [10], the values of K_r does not affect by the wave period in terms of d/L_i. The agreement between the three studies is acceptable in predicting K_r for vertical plane seawalls. Also, the figure shows that the values of K_r decrease as d/L_i increase for serrated seawalls presented in the present study (i.e. vertical rectangular serrated seawall, s/w=2.0, and vertical triangular serrated seawall, s/w=2.0) and serrated and dentated seawalls presented by [10].

4. Conclusions

The hydrodynamic performance of both vertical and sloped plane, rectangular serrated, triangular serrated, slotted, slotted with triangular serrations seawalls were investigated experimentally in terms of wave reflection coefficient, k_r using physical model studies. Based on both the dimensional analysis and measurements, predictive formulae are proposed to predict the reflection coefficient due to regular waves for the all the tested models.
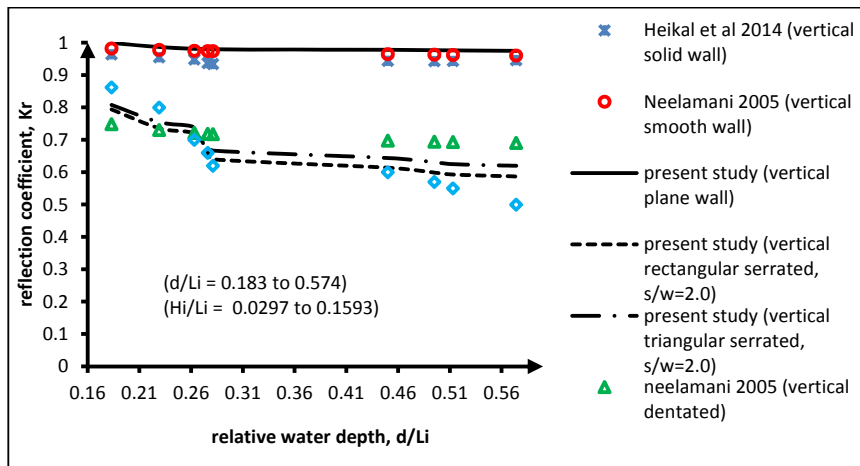

Fig (5). Comparison between the present study (vertical plane smooth wall and serrated wall) with previous works for wave reflection coefficient versus relative water depth.

The developed formulae in this paper are compared with experimental and theoretical results obtained by different authors and giving a reasonable agreement.

The results might be used for a better hydrodynamic design of vertical structures (i.e. quay walls in harbors, vertical seawalls, caisson type breakwaters) and sloped structures (i.e. seawalls, dikes, wave absorbers in the laboratory).

Acknowledgements

References

[1] H.-B. Chen, C.-P. Tsai, and J.-R. Chiu, "Wave reflection from vertical breakwater with porous structure," *Ocean Eng.*, vol. 33, no. 13, pp. 1705–1717, 2006.

[2] P. Lin and S. A. Karunarathna, "Numerical study of solitary wave interaction with porous breakwaters," *J. Waterw. Port, Coastal, Ocean Eng.*, vol. 133, no. 5, pp. 352–363, 2007.

[3] B. Zanuttigh and J. W. van der Meer, "Wave reflection from coastal structures in design conditions," *Coast. Eng.*, vol. 55, no. 10, pp. 771–779, 2008.

[4] I. Theocharis, E. N. Anastasaki, C. I. Moutzouris, and T. Giantsi, "A new wave absorbing quay-wall for wave height reduction in a harbor basin," *Ocean Eng.*, vol. 38, no. 17, pp. 1967–1978, 2011.

[5] A. S. Koraim, E. M. Heikal, and A. A. Abo Zaid, "Hydrodynamic characteristics of porous seawall protected by submerged breakwater," *Appl. Ocean Res.*, vol. 46, pp. 1–14, 2014.

[6] A. Führböter, "Wave loads on sea dikes and sea-walls," *Abbott, MB; Price, WA Coastal, Estuarial Harb. Eng. Ref. Book, London/Glasgow, England,* pp. 351–367, 1994.

[7] A. S. Koraim and O. S. Rageh, "Hydrodynamic performance of vertical porous structures under regular waves," *China Ocean Eng.*, vol. 27, no. 4, pp. 451–468, 2013.

[8] R. A. Dalrymple, M. A. Losada, and P. A. Martin, "Reflection and transmission from porous structures under oblique wave attack," *J. Fluid Mech.*, vol. 224, pp. 625–644, 1991.

[9] R. Levesque, "SPSS Inc.(2006)," *SPSS Program. data Manag. 3rd Ed. SPSS institute. USA*, 2006.

[10] S. Neelamani and N. Sandhya, "Surface roughness effect of vertical and sloped seawalls in incident random wave fields," *Ocean Eng.*, vol. 32, no. 3, pp. 395–416, 2005.